

# Homework 3 (Tasks 1-19) in EL2450 Hybrid and Embedded Control Systems

Rene Garcia	Daniel Skott	Joel Aggefors
20010124-5512	20020314-5214	20030301-4575
reneogt@kth.se	dskott@kth.se	joelag@kth.se

Jenis Jain	First name5	Last name5
20030424-T490	person number	
jjjain@kth.se	email	

February 27, 2026

## **Task 1: Compute $u_r$ and $u_l$ from $(v, \omega)$**

The robot inputs are defined as :

$$v = \frac{u_r + u_l}{2}, \quad \omega = u_r - u_l. \quad (1)$$

From (1), multiply the first equation by 2:

$$2v = u_r + u_l. \quad (2)$$

Now add (2) and the second equation in (1):

$$2v + \omega = (u_r + u_l) + (u_r - u_l) = 2u_r \Rightarrow u_r = v + \frac{\omega}{2}. \quad (3)$$

Similarly, subtract the second equation in (1) from (2):

$$2v - \omega = (u_r + u_l) - (u_r - u_l) = 2u_l \Rightarrow u_l = v - \frac{\omega}{2}. \quad (4)$$

Therefore, the wheel speeds corresponding to  $(v, \omega)$  are:

$$u_r = v + \frac{\omega}{2} \quad [1^\circ/s], \quad u_l = v - \frac{\omega}{2} \quad [1^\circ/s]$$

(5)

## **Task 2**

### **(a) Discretization, numbering , and atomic propositions**

**Workspace:**  $[-1.5, 1.5] \times [-1.5, 1.5]$  (meters). A discretization with  $K = 36$  gives a  $6 \times 6$  grid.

$R_6$ G,S	$R_7$ B	$R_{18}$ -	$R_{19}$ O	$R_{30}$ -	$R_{31}$ R,G,O
$R_5$ -	$R_8$ R,O	$R_{17}$ -	$R_{20}$ R	$R_{29}$ B,O	$R_{32}$ R
$R_4$ -	$R_9$ G	$R_{16}$ -	$R_{21}$ B	$R_{28}$ -	$R_{33}$ -
$R_3$ O	$R_{10}$ O	$R_{15}$ -	$R_{22}$ O	$R_{27}$ -	$R_{34}$ -
$R_2$ G	$R_{11}$ R,O	$R_{14}$ -	$R_{23}$ B	$R_{26}$ R,O	$R_{35}$ -
$R_1$ R	$R_{12}$ -	$R_{13}$ -	$R_{24}$ -	$R_{25}$ G	$R_{36}$ B

Figure 1: Workspace discretization with  $K = 36$  regions. Labels indicate where atomic propositions hold.

regions are numbered in a *column-wise snake* pattern: start at the bottom-left with  $R_1$ , go *up* in the first column, then *down* in the next column, and so on. Thus, the  $6 \times 6$  numbering is:

$R_6$	$R_7$	$R_{18}$	$R_{19}$	$R_{30}$	$R_{31}$
$R_5$	$R_8$	$R_{17}$	$R_{20}$	$R_{29}$	$R_{32}$
$R_4$	$R_9$	$R_{16}$	$R_{21}$	$R_{28}$	$R_{33}$
$R_3$	$R_{10}$	$R_{15}$	$R_{22}$	$R_{27}$	$R_{34}$
$R_2$	$R_{11}$	$R_{14}$	$R_{23}$	$R_{26}$	$R_{35}$
$R_1$	$R_{12}$	$R_{13}$	$R_{24}$	$R_{25}$	$R_{36}$

**Atomic propositions:** Let  $AP = \{\text{red}, \text{blue}, \text{green}, \text{obstacle}\}$ . The propositions are specified by the following positions (meters):

- **obstacle** centers (spheres of radius 0.05 m) at:

$$(-0.75, 0.75), (0.25, 1.25), (0.75, 0.75), (0.25, -0.25), (0.75, -0.75), (-0.75, -0.75), (-0.75, -0.25)$$

- **red** holds at:

$$(-0.75, 0.7), (0.2, 0.7), (1.25, 1.25), (1.2, 0.8), (0.8, -0.8), (-0.9, -0.8), (-1.25, -1.25).$$

- **blue** holds at:

$$(-0.75, 1.4), (0.9, 0.9), (0.3, 0.2), (0.25, -0.75), (1.2, -1.4).$$

- **green** holds at:

$$(-1.23, 1.25), (1.25, 1.25), (-0.9, 0.2), (-1.2, -0.7), (0.6, -1.2).$$

**Labeling rule:** a proposition is true in the region that contains its given position, i.e.

$$p \in L(R_i) \iff (x_p, y_p) \in R_i, \quad p \in AP.$$

The start position is  $(-1.25, 1.25)$ , hence  $S_0 = \{R_6\}$ .

### (b) Cell size $dx, dy$

Since the side length is 3 m and there are 6 cells per side,

$$dx = \frac{3}{6} = 0.5 \text{ m}, \quad dy = \frac{3}{6} = 0.5 \text{ m}.$$

### (c) Comment on the choice $K = 36$

A  $6 \times 6$  grid provides a finer abstraction than coarse grids (better separation of obstacles/colored areas), but increases the number of states and transitions compared to smaller  $K$ .

### (d) Transition system $T = (S, S_0, \Sigma, \rightarrow, AP, L)$

$$S = \{R_1, \dots, R_{36}\}, \quad S_0 = \{R_6\}, \quad \Sigma = \{\text{Up, Down, Left, Right}\}, AP = \{\text{red, blue, green, obstacle}\}.$$

The transition relation  $\rightarrow$  is the 4-neighborhood relation on the grid:

$$R_i \xrightarrow{\sigma} R_j \iff R_j \text{ is the adjacent region to } R_i \text{ in direction } \sigma \in \Sigma.$$

The labeling function  $L : S \rightarrow 2^{AP}$  is defined using the point-in-region rule above.

## Task 3: Find an infinite path satisfying the specification

**Specification:** (i) visit **red** infinitely often, (ii) whenever the robot is in a **red** region, the *next* region is **blue**, (iii) never enter a region labeled **obstacle**.

**Chosen red–blue pair:** From the labeling in Task 2,  $R_{20} \in \text{red}$  and  $R_{21} \in \text{blue}$ , and they are adjacent in the  $6 \times 6$  grid ( $R_{21}$  is directly below  $R_{20}$ ). Moreover,  $R_{20}, R_{21} \notin \text{obstacle}$ .

**A valid infinite path:** Starting from  $S_0 = \{R_6\}$ , one feasible prefix to reach  $R_{20}$  without entering obstacles is

$$R_6 \rightarrow R_7 \rightarrow R_{18} \rightarrow R_{17} \rightarrow R_{16} \rightarrow R_{21} \rightarrow R_{20}.$$

Then, repeat the 2-cycle  $(R_{20}, R_{21})$  forever:

$$\pi = \underbrace{(R_6, R_7, R_{18}, R_{17}, R_{16}, R_{21}, R_{20})}_{\text{prefix}} \cdot \underbrace{(R_{21}, R_{20})^\omega}_{\text{suffix repeated forever}}.$$

**Why  $\pi$  satisfies the specification:**

- $\pi$  visits  $R_{20}$  infinitely often, and  $R_{20} \in \text{red}$ , hence **red** is visited infinitely often.
- Every time  $\pi$  is in  $R_{20}$  (a **red** region), the next state is  $R_{21}$  and  $R_{21} \in \text{blue}$ , so the “after **red** next is **blue**” condition holds.
- All regions used in  $\pi$  are chosen outside the set of **obstacle** regions, hence obstacles are never entered.

## Task 4

The hybrid strategy prevents entering unintended regions by separating the motion into two simple phases. First, the robot uses a rotation mode with (approximately) zero forward speed, i.e.,  $v \approx 0$ , so it turns in place to align its heading with the straight line connecting the center of the current region to the center of the target (neighbor) region. Because the robot does not translate during this phase, it stays close to the current region center and does not drift into adjacent regions. Second, the robot switches to a line-following mode and drives forward while tracking that same center-to-center line. For neighboring regions, this line segment lies within the union of the two adjacent cells. Therefore, if the tracking error is kept small, the robot remains inside only the current and target regions during the transition, and it avoids passing through any other region that could contain an obstacle.

## Task 5

During the rotation mode, the controller is

$$\omega[k] = K_{\Psi,1}(\theta_R - \theta[k]). \quad (6)$$

The robot yaw dynamics satisfy

$$\dot{\theta}(t) = \frac{R}{L} \omega(t) \quad [1^\circ/s]. \quad (7)$$

Using forward Euler discretization with sampling time  $h$ ,

$$\theta[k+1] = \theta[k] + h \frac{R}{L} \omega[k]. \quad (8)$$

Substituting (6) into (8) and defining the error  $e[k] = \theta_R - \theta[k]$ , we obtain

$$e[k+1] = \left(1 - \frac{hR}{L} K_{\Psi,1}\right) e[k]. \quad (9)$$

For asymptotic stability of the discrete-time error dynamics, we require

$$\left|1 - \frac{hR}{L} K_{\Psi,1}\right| < 1 \iff 0 < \frac{hR}{L} K_{\Psi,1} < 2 \iff \boxed{0 < K_{\Psi,1} < \frac{2L}{hR}}. \quad (10)$$

A practical choice is to pick  $K_{\Psi,1}$  well inside this interval (e.g.,  $K_{\Psi,1} = \alpha \frac{L}{hR}$  with  $\alpha \in (0, 1)$ ) to avoid oscillations and actuator saturation.

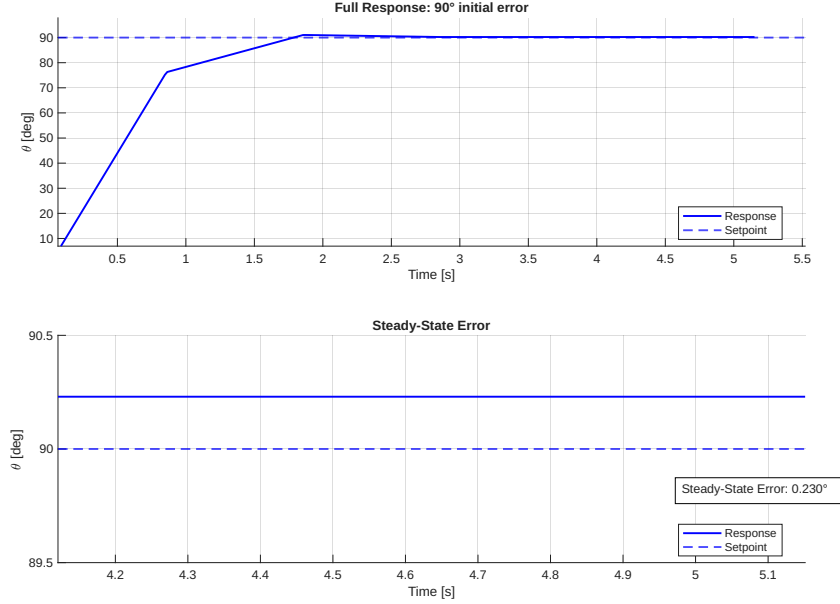
## Task 6

First we define the proportional constant value. Given eq. (10), we could aim for a deadbeat controller by setting  $K_{\Psi,1} = \frac{2L}{hR}$ , nonetheless, this would force the controller to correct the error in one sampling step, completely ignoring physical limits and inertia. A safer value to chose is the middle of the stability range:

$$K_{\Psi,1} = \frac{1}{2} \frac{2L}{hR} = \frac{L}{hR} = \frac{0.16}{0.033 * 1} = 4.85 \quad [1/s]. \quad (11)$$

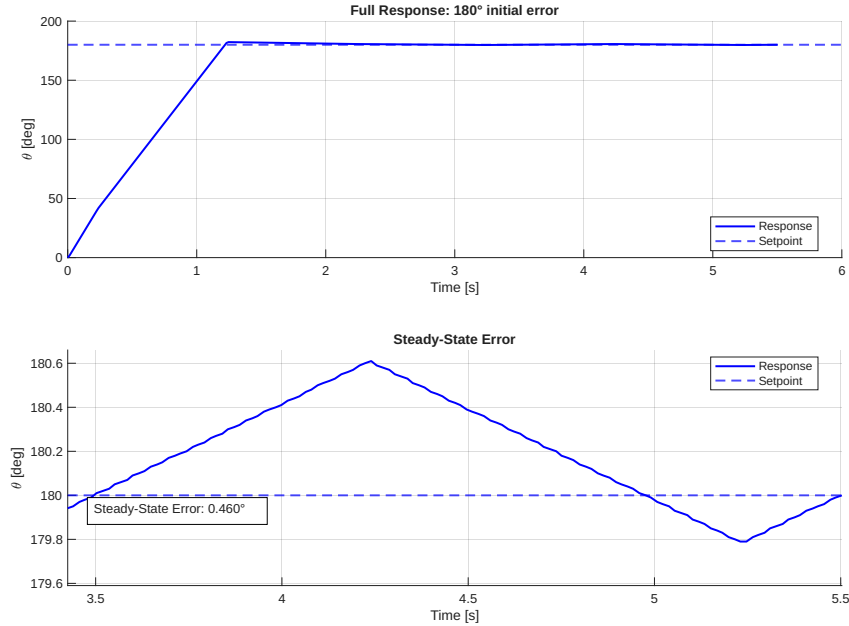
To test the performance of the controller, we run 2 different scenarios:

- Scenario 1:  $\theta_R = 90^\circ$ ,  $\theta[0] = 0^\circ$  (90 degree turn)



For this case, the wheels stop turning at around  $1.85\text{ s}$ , and there is a **steady-state** error of  $0.23^\circ$ .

- Scenario 2:  $\theta_R = 180^\circ$ ,  $\theta[0] = 0^\circ$  (180 degree turn)



For this case, there is a constant ripple that slowly rotates the robot back and forth around the target angle. This is a case of limit cycle caused by quantization. For this case, we consider the largest error, that is, the peak of the ripple. Then, the **steady-state** error is  $0.46^\circ$ .

In general, can see that the controller **asymptotically stabilizes** the error in both scenarios, as we don't see divergence over time.

## Task 7

Assume  $\theta[k+1] = \theta[k] = \theta$  so  $v_c = [\cos \theta \ \sin \theta]^\top$  is constant and  $v_c^\top v_c = 1$ . Using  $\dot{p} = Rvv_c$  with  $p = [x \ y]^\top$  and forward Euler,

$$p[k+1] = p[k] + hRv[k]v_c \Rightarrow \Delta_0[k+1] = \Delta_0[k] - hRv[k]v_c.$$

Premultiplying by  $v_c^\top$  yields

$$d_0[k+1] = v_c^\top \Delta_0[k+1] = d_0[k] - hRv[k].$$

With  $v[k] = K_{\omega,1}d_0[k]$ ,

$$d_0[k+1] = (1 - hRK_{\omega,1})d_0[k].$$

Asymptotic stability requires  $|1 - hRK_{\omega,1}| < 1$ , hence

$$\boxed{0 < K_{\omega,1} < \frac{2}{hR}}.$$

## Task 8

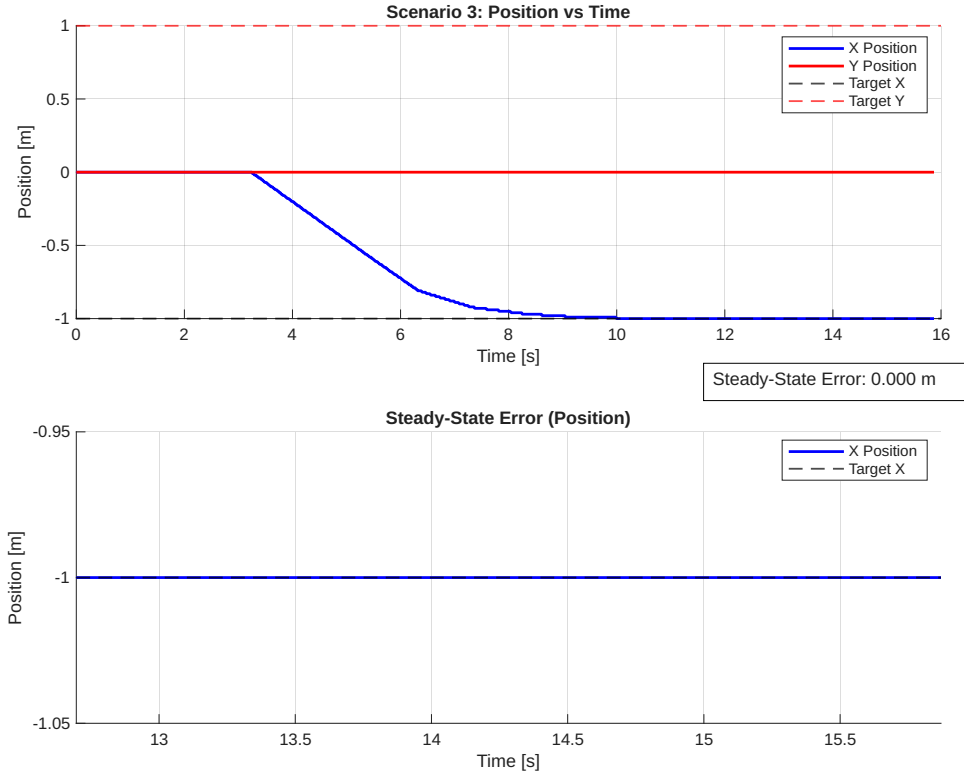
Similarly to Task 6, we select  $K_{\omega,1}$  in the middle of the stability interval:

$$K_{\omega,1} = \frac{1}{2} \frac{2}{hR} = \frac{1}{hR} = \frac{1}{0.033 * 1} = 30.3 \quad [\frac{1}{m \cdot s}]. \quad (12)$$

To test the performance of the controller, we run 1 single scenario:

- **Scenario 1: Diagonal Error**

Starting position:  $(x_0, y_0) = (0, 0)$ ,  $\theta = 0^\circ$  Target:  $(x_g, y_g) = (-1, 1)$

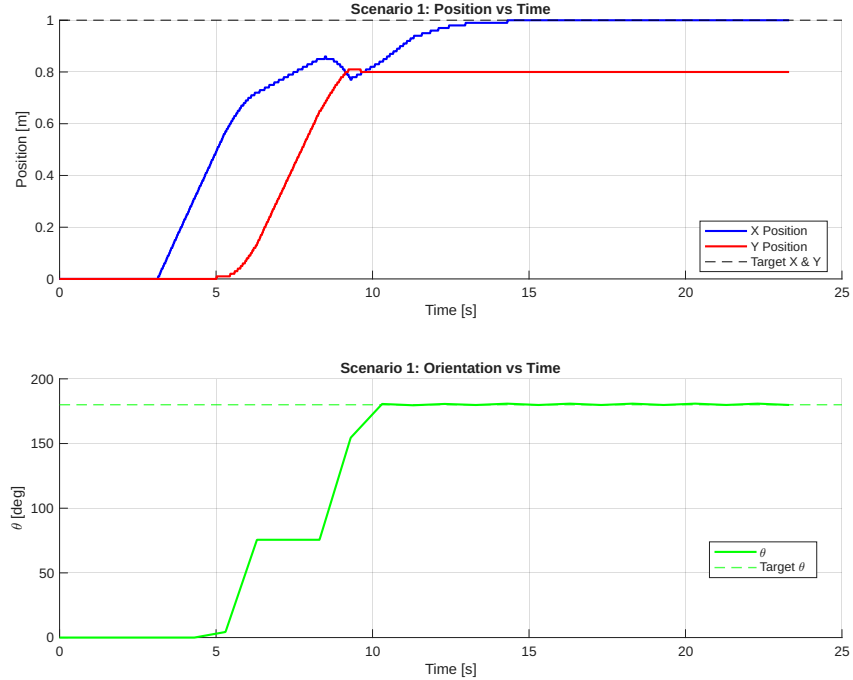


As we can see, the robot moves only in the  $x$  direction, as this is the direction it is facing initially. The controller successfully reduces the X error to zero, but the Y error remains, therefore, **We conclude that it is not possible to ensure that  $[x[k], y[k]]^T$  stays exactly at  $[x_0, y_0]^T$  for any initial orientation.**

## Task 9

To test both controllers together, we simulate an scenario where we have error in the position and angle, and enable both controllers.

- **Scenario 1:** Starting position:  $(x_0, y_0) = (0, 0)$ ,  $\theta = 0^\circ$  Target:  $(x_g, y_g) = (1, 1)$ ,  $\theta^R = 180^\circ$



As we can see, the angle error is completely corrected first, thus blocking the possibility of correcting the position error. **In conclusion, there is a cross-coupling effect between the rotational and translational dynamics.**

## Task 10

Assume  $\theta[k] = \theta_g$ , hence  $v_g = [\cos \theta_g \quad \sin \theta_g]^\top$  is constant and  $v_g^\top v_g = 1$ . With  $\dot{p} = Rvv_g$  and forward Euler,

$$p[k+1] = p[k] + hRv[k]v_g \Rightarrow \Delta_g[k+1] = \Delta_g[k] - hRv[k]v_g.$$

Premultiplying by  $v_g^\top$  yields

$$d_g[k+1] = v_g^\top \Delta_g[k+1] = d_g[k] - hRv[k].$$

Using  $v[k] = K_{\omega,2}d_g[k]$ ,

$$d_g[k+1] = (1 - hRK_{\omega,2})d_g[k].$$

Asymptotic stability requires  $|1 - hRK_{\omega,2}| < 1$ , hence

$$0 < K_{\omega,2} < \frac{2}{hR}.$$

A practical choice is to select  $K_{\omega,2}$  well inside this interval (e.g.,  $K_{\omega,2} = \alpha \frac{1}{hR}$  with  $\alpha \in (0, 1)$ ) to ensure monotone convergence and robustness to discretization/actuator limits.

## Task 11

The closed-loop dynamics of  $d_g$  are

$$d_g[k+1] = (1 - HRK_{\omega,2})d_g[k].$$

For  $0 < HRK_{\omega,2} < 2$ , we have  $|1 - HRK_{\omega,2}| < 1$ , hence

$$\lim_{k \rightarrow \infty} d_g[k] = 0.$$

Thus,  $d_g$  is asymptotically stabilized in 0.

However, since  $\omega[k] = 0$ , the orientation  $\theta$  remains constant and the robot moves along a fixed straight line. If the initial orientation is not aligned with the goal direction, the robot cannot correct lateral error. Therefore,

$$[x[k], y[k]]^T \not\rightarrow [x_g, y_g]^T$$

for arbitrary initial orientations.

In Fig. 2 we can see that the robot travels in a straight line and that it comes closer to the goal. Another observation not observable in the graph is that the robot slows down and stops at the goal.

## Task 12

The controller for line-following (part II) is

$$\omega[k] = K_{\Psi,2} d_p[k].$$

Assume the robot is on the line from  $(x_0, y_0)$  to  $(x_g, y_g)$  and  $\theta$  is close to  $\theta_g$  so that

$$d_p[k] \approx p(\theta_g - \theta[k]), \quad p > 0.$$

Let  $e[k] = \theta_g - \theta[k]$ , hence  $d_p[k] \approx p e[k]$ . From the yaw dynamics  $\dot{\theta} = \frac{R}{L}\omega$  and forward Euler with sampling time  $h$ ,

$$\theta[k+1] = \theta[k] + h \frac{R}{L} \omega[k].$$

Therefore,

$$e[k+1] = \theta_g - \theta[k+1] = e[k] - h \frac{R}{L} \omega[k] = e[k] - h \frac{R}{L} K_{\Psi,2} d_p[k] \approx \left(1 - h \frac{R}{L} K_{\Psi,2} p\right) e[k].$$

Multiplying by  $p$  gives the discrete-time dynamics of  $d_p$ :

$$d_p[k+1] \approx \left(1 - h \frac{R}{L} K_{\Psi,2} p\right) d_p[k].$$

Thus  $d_p[k]$  is asymptotically stabilized in 0 iff

$$\left|1 - h \frac{R}{L} K_{\Psi,2} p\right| < 1 \iff 0 < K_{\Psi,2} < \frac{2L}{hRp}.$$

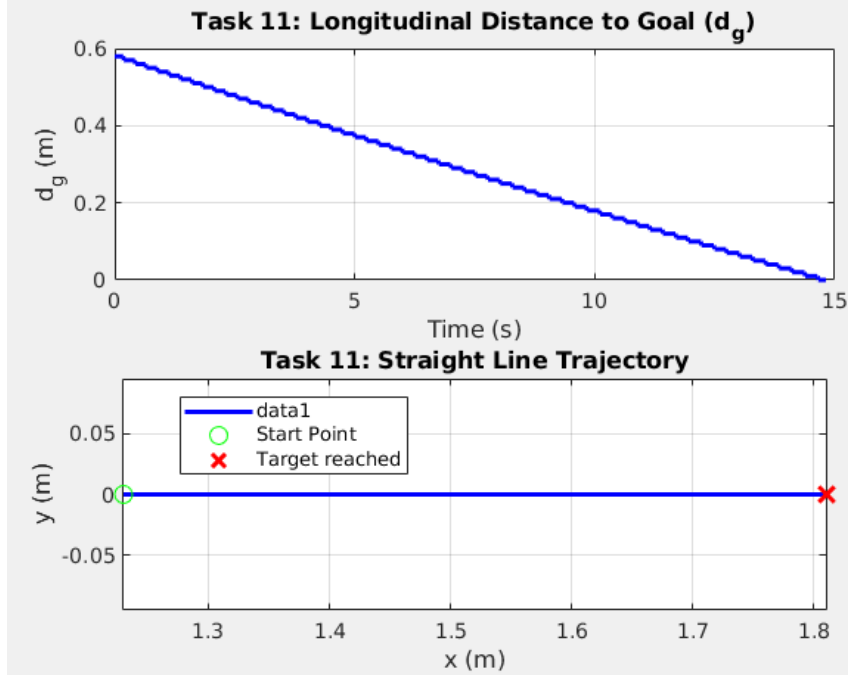


Figure 2: Result from discrete straight line controller

**Choice of  $K_{\Psi,2}$ .** Select  $K_{\Psi,2}$  strictly inside the stability interval, e.g.

$$K_{\Psi,2} = \alpha \frac{L}{hRp}, \quad \alpha \in (0, 1),$$

which yields the contraction factor  $1 - \alpha$  (monotone convergence) and keeps the closed-loop behavior consistent when the sampling time  $h$  changes.

## Task 13

If we model the corrective input using the (nonlinear) sine term, for instance

$$d_p \approx p \sin(\theta_g - \theta),$$

then  $p$  plays the role of a proportional gain. Increasing  $p$  improves the tracking accuracy of  $\theta$  to the goal  $\theta_g$ . However, if  $p$  is chosen too large the closed-loop trajectory typically oscillates around  $\theta_g$  and cannot settle at a point. Intuitively this happens because the region of attraction (the set of initial conditions that converge to  $\theta_g$ ) shrinks as  $p$  increases, so overly large gains reduce stability margins and promote sustained oscillations.

**Remark.** In particular one must not replace  $\sin(\theta_g - \theta)$  by  $\theta_g - \theta$  unless the small-angle approximation is explicitly justified.

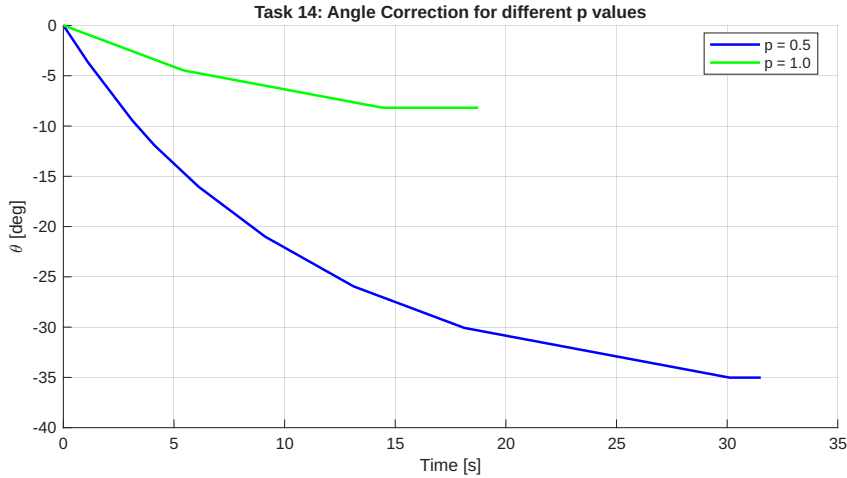
## Task 14

From Task 12, the stability condition for the line-following controller is

$$0 < K_{\Psi,2} < \frac{2L}{hRp}.$$

Since  $p$  appears in the denominator, a larger  $p$  shrinks the stability interval and reduces the maximum admissible gain  $K_{\Psi,2}$ . We compare two values experimentally:

- $p = 0.5$ : stability bound  $K_{\Psi,2} < \frac{2 \cdot 0.16}{1 \cdot 0.033 \cdot 0.5} \approx 19.4$ . The wide stability margin allows a strong corrective input without oscillations. The measured displacement error is  $y_{\text{err}} = 0.1 \text{ m}$ .
- $p = 1.0$ : stability bound  $K_{\Psi,2} < \frac{2 \cdot 0.16}{1 \cdot 0.033 \cdot 2} \approx 4.85$ . The narrow margin means the same gain  $C$  pushes the system closer to the stability boundary, resulting in slower or oscillatory convergence. The measured displacement error is  $y_{\text{err}} = 0.5 \text{ m}$ .



As can be seen in the plot,  $p = 0.5$  provides a smoother and faster convergence to the target angle  $\theta_g = 90^\circ$ , while  $p = 1.0$  leads to a noticeably slower response with a larger displacement error. Therefore, we choose  $p = 0.5$  because it offers a wider stability margin, better transient behavior, and a significantly smaller steady-state displacement error.

## Task 15

Solution to the task

## Task 16 : Hybrid automaton

Define the hybrid automaton  $H = (Q, X, \text{Init}, f, D, E, G, R)$ .

**Discrete states.**

$$Q = \{q_{\text{rot}}, q_{\text{line}}\},$$

where  $q_{\text{rot}}$  aligns the robot with the goal direction and  $q_{\text{line}}$  performs line-following / go-to-goal.

**Continuous state and initialization.**

$$X = \begin{bmatrix} x \\ y \\ \theta \end{bmatrix}, \quad \text{Init} = \left\{ (q_{\text{rot}}, X) \mid X = \begin{bmatrix} x_s \\ y_s \\ \theta_s \end{bmatrix} \right\}.$$

**Continuous dynamics (closed-loop).** Robot kinematics:

$$\dot{x} = R v \cos \theta, \quad \dot{y} = R v \sin \theta, \quad \dot{\theta} = \frac{R}{L} \omega.$$

Let  $\theta_R = \text{atan2}(y_g - y, x_g - x)$ .

Mode  $q_{\text{rot}}$ :

$$\omega = K_{\Psi,1}(\theta_R - \theta), \quad v = K_{\omega,1}d_0.$$

Mode  $q_{\text{line}}$ :

$$v = K_{\omega,2}d_g, \quad \omega = K_{\Psi,2}d_p.$$

### Domains.

$$D(q_{\text{rot}}) = D(q_{\text{line}}) = \mathbb{R}^2 \times (-180^\circ, 180^\circ].$$

### Edges and guards.

$$E = \{(q_{\text{rot}}, q_{\text{line}}), (q_{\text{line}}, q_{\text{rot}})\}.$$

Using thresholds  $\varepsilon_\theta > 0$  and  $\varepsilon_g > 0$ :

$$G(q_{\text{rot}}, q_{\text{line}}) = \{X : |\theta_R - \theta| \leq \varepsilon_\theta\}, \quad G(q_{\text{line}}, q_{\text{rot}}) = \{X : \|(x_g - x, y_g - y)\| \leq \varepsilon_g\}.$$

**Resets.** No state jump at switching (identity reset):

$$R(q_{\text{rot}}, q_{\text{line}}) : X^+ = X, \quad R(q_{\text{line}}, q_{\text{rot}}) : X^+ = X.$$

(If multiple waypoints are used, the next goal  $(x_g, y_g)$  is updated externally when  $\varepsilon_g$  is reached.)

## Task 17

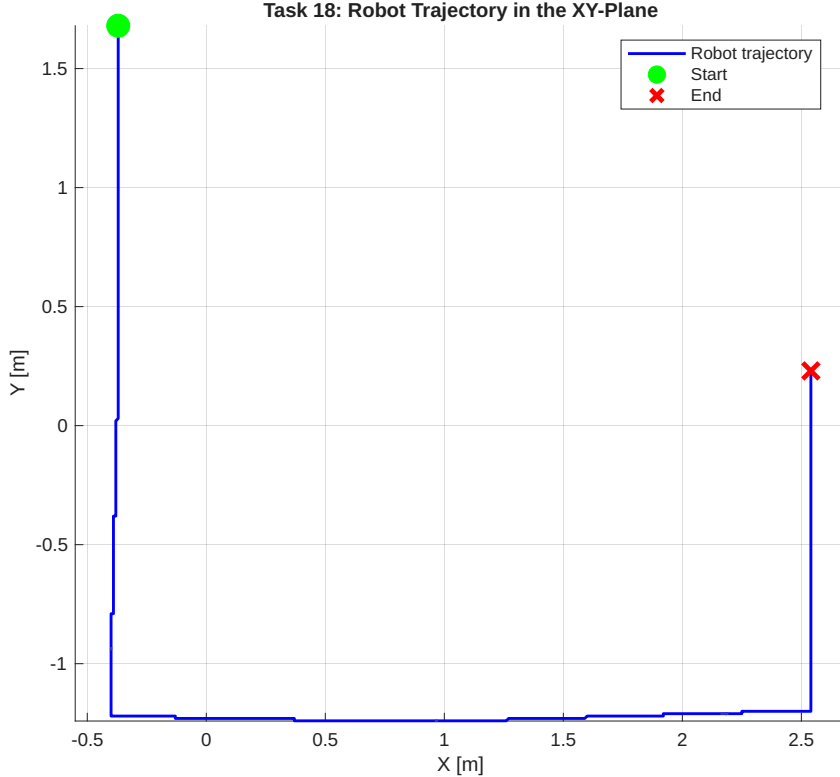
Solution to the task

## Task 18

We execute the plan derived in Task 3 on the online simulator by programming the sequence of waypoints corresponding to the region centers along the path

$$R_6 \rightarrow R_7 \rightarrow R_{18} \rightarrow R_{17} \rightarrow R_{16} \rightarrow R_{21} \rightarrow R_{20} \rightarrow (R_{21}, R_{20})^\omega.$$

Each waypoint is the center  $(x_c, y_c)$  of the respective  $0.5 \times 0.5$  m region. The hybrid automaton from Task 16 handles transitions between waypoints: the robot first rotates in place ( $q_{\text{rot}}$ ) to align with the next waypoint, then drives in a straight line ( $q_{\text{line}}$ ) while the line-following controller corrects lateral deviations.



### Observations:

- The trajectory consists of clearly distinguishable straight-line segments connected by sharp turns at each waypoint, confirming that the rotate-then-drive strategy from Task 4 works as intended.
- The robot successfully follows the planned prefix path and reaches the  $R_{20} \leftrightarrow R_{21}$  cycle, satisfying the specification (visit red infinitely often, always followed by blue, no obstacles entered).
- Small lateral offsets are visible along the straight segments due to the finite sampling time and the discrete nature of the controller, but these remain well within the 0.5 m cell width, so the robot does not enter unintended regions.
- At each waypoint the robot dwells briefly while rotating, which introduces a slight position drift. This is acceptable as long as the drift stays inside the current region.

## Task 19

During each transition between two adjacent regions  $R_i$  and  $R_j$ , the safety property requires that the robot remains inside  $R_i \cup R_j$  at all times. Whether this holds depends directly on how well the continuous controllers perform in each mode of the hybrid automaton.

**Rotation mode ( $q_{\text{rot}}$ ).** While rotating in place, the robot should ideally have  $v = 0$  so that it does not translate. In practice, the controller from Task 5 sets  $v = K_{\omega,1}d_0$ , which is nonzero whenever there is a position error. If the rotation is slow (small  $K_{\Psi,1}$ ) or the

sampling time  $h$  is large, the robot spends many steps turning and may drift due to this residual forward velocity. A large steady-state orientation error (as observed in Task 6) also means the robot enters the line-following mode with a heading offset, causing it to initially deviate from the intended straight path. Both effects can push the robot outside  $R_i$  during the rotation phase if the drift exceeds  $dx/2 = 0.25$  m.

**Line-following mode ( $q_{\text{line}}$ ).** The lateral tracking error  $d_p$  determines how far the robot deviates from the center-to-center line connecting  $R_i$  and  $R_j$ . From Task 12,  $d_p$  converges to zero only if  $0 < K_{\Psi,2} < \frac{2L}{hRp}$ . A gain close to the stability boundary leads to oscillatory convergence, and the transient lateral excursions may exceed the cell half-width. Furthermore, the choice of  $p$  directly affects the magnitude of  $d_p$ : as shown in Task 14,  $p = 2$  produced a lateral error of 0.5 m, which equals the full cell width and would violate the safety property. Conversely,  $p = 0.5$  kept the error at 0.1 m, well within bounds.

**Switching thresholds.** The guard  $\varepsilon_\theta$  for the rotation-to-line transition also matters: a loose threshold means the robot starts driving forward while still significantly misaligned, producing a large initial  $d_p$ . Similarly, the goal threshold  $\varepsilon_g$  determines how close to the waypoint center the robot is when it begins rotating toward the next target. A large  $\varepsilon_g$  means the robot starts the next rotation far from the region center, increasing the risk of drifting into a third region.

**Summary.** The safety property is preserved when (i) the rotation controller converges fast enough that positional drift during turning is small, (ii) the line-following controller keeps lateral deviations well below  $dx/2$ , and (iii) the switching thresholds  $\varepsilon_\theta$  and  $\varepsilon_g$  are chosen tight enough that the robot is well-aligned and well-centered at each mode switch. In our implementation, the gains  $K_{\Psi,1} = L/(hR)$  and  $K_{\Psi,2} = \alpha L/(hRp)$  with  $p = 0.5$  satisfy these requirements, as confirmed by the trajectory in Task 18 staying within the intended regions.

## References

- [1] Hassan K Khalil. *Nonlinear systems*. Prentice Hall, Upper Saddle river, 3. edition, 2002. ISBN 0-13-067389-7.
- [2] Tobias Oetiker, Hubert Partl, Irene Hyna, and Elisabeth Schlegl. *The Not So Short Introduction to L<sup>A</sup>T<sub>E</sub>X 2<sub>&</sub>*. Oetiker, OETIKER+PARTNER AG, Aarweg 15, 4600 Olten, Switzerland, 2008. <http://www.ctan.org/info/lshort/>.
- [3] Shankar Sastry. *Nonlinear systems: analysis, stability, and control*, volume 10. Springer, New York, N.Y., 1999. ISBN 0-387-98513-1.